Novel Antimony/Aluminum/Carbon Nanocomposite for High-Performance Rechargeable Lithium Batteries

Cheol-Min Park and Hun-Joon Sohn*

Department of Materials Science and Engineering, Research Center for Energy Conversion and Storage, Seoul National University, Seoul, 151-742, Korea

Received January 15, 2008. Revised Manuscript Received March 3, 2008

A simple method of transforming micrometer-sized Al and Sb powders into a new nanocomposite modified with carbon by the alloying reaction of Al and Sb to form the AlSb phase and the dealloying reaction of the AlSb phase with carbon to synthesize the $Sb/Al_4C_3/C$ nanocomposite was developed using a high-energy mechanical milling technique. The $Sb/Al_4C_3/C$ nanocomposite was confirmed, using various analytical techniques, to be composed of a reduced crystalline Sb phase, amorphous Al_4C_3 phase, and amorphous carbon. This novel nanocomposite showed a highly reversible reaction with Li, a high capacity of 687 mAh g^{-1} with a good Coulombic efficiency of 85% for the first cycle, and a high capacity retention above 520 mAh g^{-1} over 200 cycles. Additionally, by controlling the voltage window, an excellent cyclability with a high rate capability also was achieved. These excellent electrochemical properties demonstrated by the $Sb/Al_4C_3/C$ nanocomposite electrode confirm its potential as a new alternative anode material for Li-ion batteries.

Introduction

Rechargeable solid-state batteries, such as nickel−cadmium, nickel−metal hydride, or Li-ion, can be considered as the heart of the portable power source market. In particular, rechargeable Li-ion batteries are a promising choice for hybrid electric vehicles and various portable electronics. At present, graphite (LiC_6: 372 mAh g^{-1}) is used as the anode material for lithium-ion batteries,[1–3] but ongoing research efforts have been focused on enhancing the high-energy density, good cyclability, and high rate capability of lithium-ion batteries. Among the many possible alternatives, much effort has been devoted to lithium alloys such as tin ($Li_{4.4}Sn$: 993 mAh g^{-1}),[4–6] silicon ($Li_{4.4}Si$: 4198 mAh g^{-1}),[7–9] aluminum (LiAl: 993 mAh g^{-1}),[10,11] phosphorus (Li_3P: 2596 mAh g^{-1}),[12–14] antimony (Li_3Sb: 660 mAh g^{-1}),[15–17] and magnesium ($Li_{11}Mg_3$: 4077 mAh g^{-1})[18] based systems due to their ability to react reversibly with large amounts of Li per formula unit. Although Li alloy based systems have a higher energy density, they suffer from poor capacity retention due to the failure of active materials caused by a large volume change during the charge/discharge processes.

Nanostructured and nanocomposite materials[19–21] have attracted a large amount of attention due to their wide applications in various fields including lithium batteries, fuel cells, solar materials, electrochemical capacitors, biosensors, etc. Among these many applications, electrode materials with a high capacity, high rate capability, and stable cycling behavior for lithium-ion batteries were studied intensively due to the ability of these materials to provide a higher interfacial area, increase the lithium-ion diffusion rate, and accommodate the strain generated during cycling. Particularly, nanocomposites modified with carbon can be considered to be a practical solution for alloying anodes. The detrimental effect due to the aggregation of nanosized metal particles, caused by a high surface reactivity, can be minimized using finely dispersed, nanosized, metallic particles in the carbon matrix. Although many studies demon-

* Corresponding author. E-mail: hjsohn@snu.ac.kr.

(1) Dahn, J. R.; Zheng, T.; Liu, Y.; Xue, J. S. *Science (Washington, DC, U.S.)* **1995**, *270*, 590.
(2) Winter, M.; Besenhard, J. O.; Spahr, M. E.; Novak, P. *Adv. Mater.* **1998**, *10*, 725.
(3) Yoshio, M.; Wang, H.; Fukuda, K. *Angew. Chem., Int. Ed.* **2003**, *42*, 4203.
(4) Idota, Y.; Kubota, T.; Matsufuji, A.; Maekawa, Y.; Miyasaka, T. *Science (Washington, DC, U.S.)* **1997**, *276*, 1395.
(5) Lou, X. W.; Wang, Y.; Yuan, C.; Lee, J. Y.; Archer, L. A. *Adv. Mater.* **2006**, *18*, 2325.
(6) Park, M.-S.; Wang, G.-X.; Kang, Y-M.; Wexler, D.; Dou, S.-X.; Liu, H.-K.; *Angew. Chem., Int. Ed.* **2007**, *46*, 750.
(7) Ng, S.-H.; Wang, J.; Wexler, D.; Konstantinov, K.; Guo, Z.-P.; Liu, H.-K. *Angew. Chem., Int. Ed.* **2006**, *45*, 6896.
(8) Larcher, D.; Mudalige, C.; George, A. E.; Porter, V.; Gharghouri, M.; Dahn, J. R. *Solid State Ionics* **1999**, *122*, 71.
(9) Wen, Z. S.; Yang, J.; Wang, B. F.; Wang, K.; Liu, Y. *Electrochem. Commun.* **2003**, *5*, 165.
(10) Wen, C. J.; Boukamp, B. A.; Huggins, R. A.; Weppner, W. *J. Electrochem. Soc.* **1979**, *126*, 2258.
(11) Jeong, G.-J.; Kim, Y.-U.; Sohn, H.-J.; Kang, T. *J. Power Sources* **2001**, *101*, 201.
(12) Park, C.-M.; Sohn, H.-J. *Adv. Mater.* **2007**, *19*, 2465.
(13) Souza, D. C. S.; Pralong, V.; Jacobson, A. J.; Nazar, L. F. *Science (Washington, DC, U.S.)* **2002**, *296*, 2012.
(14) Kim, Y.-U.; Lee, C. K.; Sohn, H.-J.; Kang, T. *J. Electrochem. Soc.* **2004**, *151*, 933.
(15) Park, C.-M.; Yoon, S.; Lee, S.-I.; Kim, J.-H.; Jung, J.-H.; Sohn, H.-J. *J. Electrochem. Soc.* **2007**, *154*, 917.
(16) Bryngelsson, H.; Eskhult, J.; Nyholm, L.; Herranen, M.; Alm, O.; Edstrom, K. *Chem. Mater.* **2007**, *19*, 1170.
(17) Honda, H.; Sakaguchi, H.; Fukuda, Y.; Esaka, T. *Mater. Res. Bull.* **2003**, *38*, 647.
(18) Park, C.-M.; Kim, Y.-U.; Kim, H.; Sohn, H.-J. *J. Power Sources* **2006**, *158*, 1451.
(19) Tarascon, J. M.; Armand, M. *Nature (London, U.K.)* **2001**, *414*, 359.
(20) Arico, A. S.; Bruce, P.; Scrosati, B.; Tarascon, J. M.; Schalkwijk, W. V. *Nat. Mater.* **2005**, *4*, 366.
(21) Derrien, G.; Hassoun, J.; Panero, S.; Scrosati, B. *Adv. Mater.* **2007**, *19*, 2336.

10.1021/cm800142n CCC: $40.75
Published on Web 04/16/2008

strated the superior cyclic performance of nanocomposite materials, most nanocomposite materials were synthesized by chemical methods,[22,23] such as reduction, sol–gel, and coprecipitation methods. However, the materials thus obtained showed a poor reversibility during the first cycle due to the presence of various impurities such as irreversible salts and oxides. Consequently, the simple synthesis of a nanocomposite with good Coulombic efficiency during the first cycle and high-capacity retention is considered to be the best solution to realize a truly high-capacity electrode material for lithium-ion batteries.

Herein, we endeavored to find a new, high-capacity, alloying anode by simple synthesis of nanocomposites and selected Al and Sb, which have an alloying phase of AlSb, as both elements react reversibly with Li. Considering the synthesis of a nanocomposite modified with carbon, we developed a simple method for transforming micrometer-sized Al and Sb powders into a new nanocomposite modified with carbon by the alloying of Al and Sb (eq 1) and dealloying (eq 2) with carbon using a high-energy mechanical milling (HEMM) technique at ambient temperature and pressure. Since the Al_4C_3 phase is thermodynamically more stable than the AlSb phase, carbon was added as a dealloying source to obtain a new nanocomposite material, as shown in the following reactions. Alloying reaction

$$Al + Sb \rightarrow AlSb \quad (\Delta G^0 = -47.721\ \text{kJ/mol, 298 K}) \quad (1)$$

Dealloying reaction

$$4AlSb + 3C \rightarrow 4Sb + Al_4C_3 \quad (\Delta G^0 = -3.682\,\text{kJ/mol, 298 K}) \quad (2)$$

Experimental Procedures

Preparation of Nanocomposite. AlSb nanopowder was prepared with Al (Kojundo, av size: 20 μm) and Sb (Aldrich, av size: 100 μm) powders using the HEMM (vibratory mill, 700 rpm) technique at ambient temperature and pressure. Al and Sb powders and stainless steel balls (diameter: 3/8 and 3/16 in.) were put into a hardened steel vial having a capacity of 80 cm^3 with a ball/powder ratio of 20:1. The HEMM process was conducted under an Ar atmosphere for 24 h. The same milling technique was employed for 12 h to produce the $Sb/Al_4C_3/C$ nanocomposite, as described previously. Preliminary studies showed that the optimum composition of AlSb/carbon (Super P) was 70:30 by wt %. The same milling technique was employed for 50 h for the Al_4C_3/C composite, as described previously, and the composition of Al_4C_3 (Aldrich, –325 mesh) to carbon (Super P) was 70:30 by wt %. To identify impurities, such as iron, elemental analysis was conducted by EDS (energy dispersive spectroscopy) attached to SEM (scanning electron microscopy, JEOL, JSM-6360), and the result showed that only 0.3 wt % iron was detected.

Materials Characterization. AlSb and $Sb/Al_4C_3/C$ nanocomposite samples were identified by X-ray diffraction (XRD, Rigaku, D-MAX2500-PC), X-ray photoelectron spectroscopy (XPS, Kratos, AXIS), and high-resolution transmission electron microscopy (HRTEM, JEOL 3000F) operating at 300 kV. For the TEM observation, a dilute suspension was dropped on a carbon- or SiO-coated TEM grid and dried.

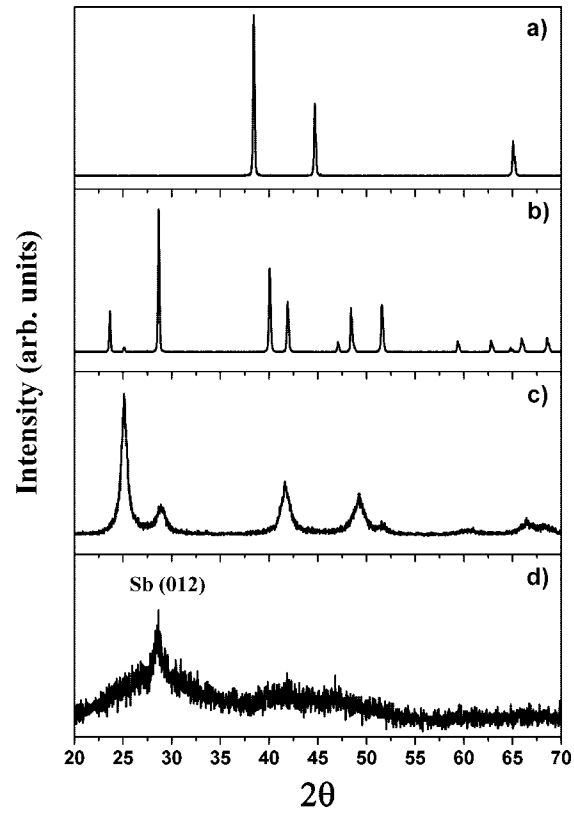

Figure 1. XRD patterns: (a) aluminum, (b) antimony, (c) AlSb, and (d) $Sb/Al_4C_3/C$ nanocomposite.

Electrochemical Measurements. For the electrochemical evaluation of the Al, Sb, AlSb, and $Sb/Al_4C_3/C$ nanocomposites, electrodes were prepared by coating slurries containing the active material (70 wt %), carbon black (Denka, 15 wt %) as a conductor, and polyvinylidene fluoride (PVDF) dissolved in *N*-methyl pyrrolidinone (NMP) as a binder (15 wt %) on copper foil substrates and pressed and dried at 120 °C for 4 h under a vacuum. Laboratory-made, coin-type, electrochemical cells were assembled in an Ar-filled glovebox using Celgard 2400 as a separator, Li foil as the counter and reference electrodes, and 1 M $LiPF_6$ in ethylene carbonate (EC)/diethyl carbonate (DEC) (1:1 by volume, Samsung) as an electrolyte. All of the cells were tested galvanostatically between 0.0 and 2.0 or 0.35 and 2.0 V versus Li/Li^+ at a current density of 100 mA g^{-1} using a Maccor automated tester. During charging, Li was inserted into the electrode, while Li was extracted from the working electrode during the discharge.

Results and Discussion

Figure 1a–d shows the XRD patterns of the Al, Sb, AlSb, and $Sb/Al_4C_3/carbon$ nanocomposite, respectively. With micrometer-sized Al and Sb powders, the AlSb phase was prepared by mechanical alloying, in which all of the peaks corresponded to AlSb and no other phases were detected. Additional mechanical alloying with carbon was performed, in which the XRD peaks displayed an amorphous phase and only a main Sb peak of (012) with a reduced crystallinity appeared.

(22) Lee, K. T.; Jung, Y. S.; Oh, S. M. *J. Am. Chem. Soc.* **2003**, *125*, 5652.
(23) Fan, J.; Wang, T.; Yu, C.; Tu, B.; Jiang, Z.; Zhao, D. *Adv. Mater.* **2004**, *16*, 1432.

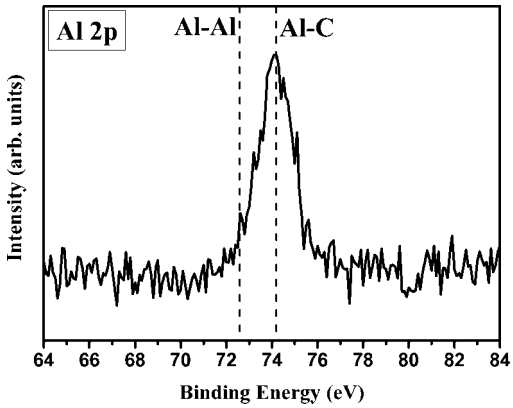

Figure 2. XPS image of Sb/Al$_4$C$_3$/C nanocomposite.

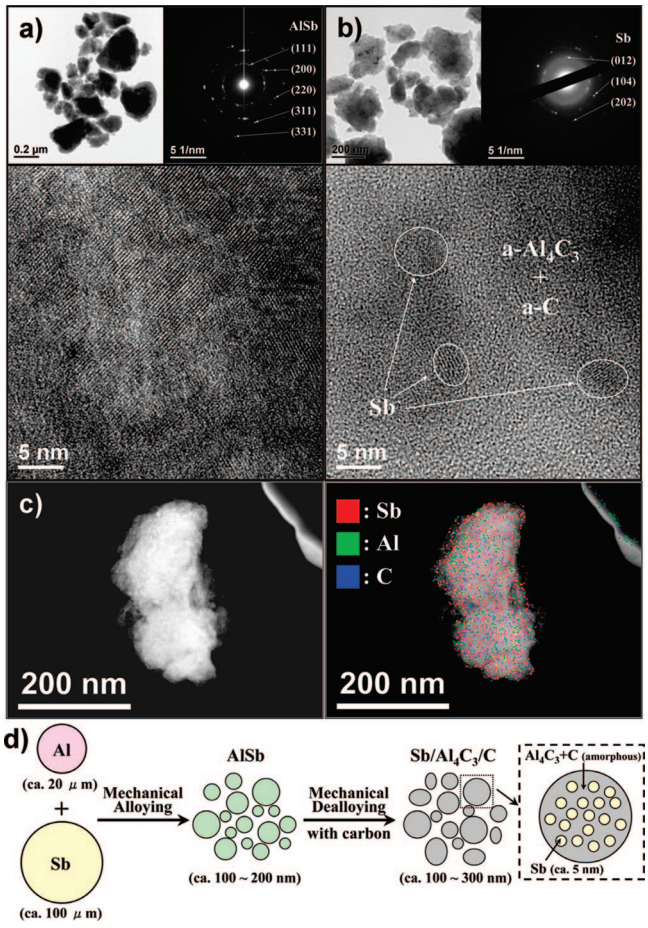

Figure 3. TEM images and corresponding lattice spacing: (a) AlSb, (b) Sb/Al$_4$C$_3$/C nanocomposite, and (c) scanning TEM (STEM) image of Sb/Al$_4$C$_3$/C nanocomposite and its EDS mapping image. (d) Schematic representation of the new Sb/Al$_4$C$_3$/C nanocomposite by mechanical alloying and dealloying.

To analyze the amorphous phase of the Sb/Al$_4$C$_3$/carbon nanocomposite, XPS analysis was conducted, and the amorphous Al$_4$C$_3$ phase (74.1 eV)[24] was detected, as shown in Figure 2. On the basis of the previous XRD and XPS analyses, the Sb/Al$_4$C$_3$/carbon nanocomposite was confirmed to be composed of a reduced crystalline Sb phase, amorphous Al$_4$C$_3$ phase, and amorphous carbon.

(24) Hinnen, C.; Imbert, D.; Siffre, J. M.; Marcus, P. *Appl. Surf. Sci.* **1994**, *78*, 219.

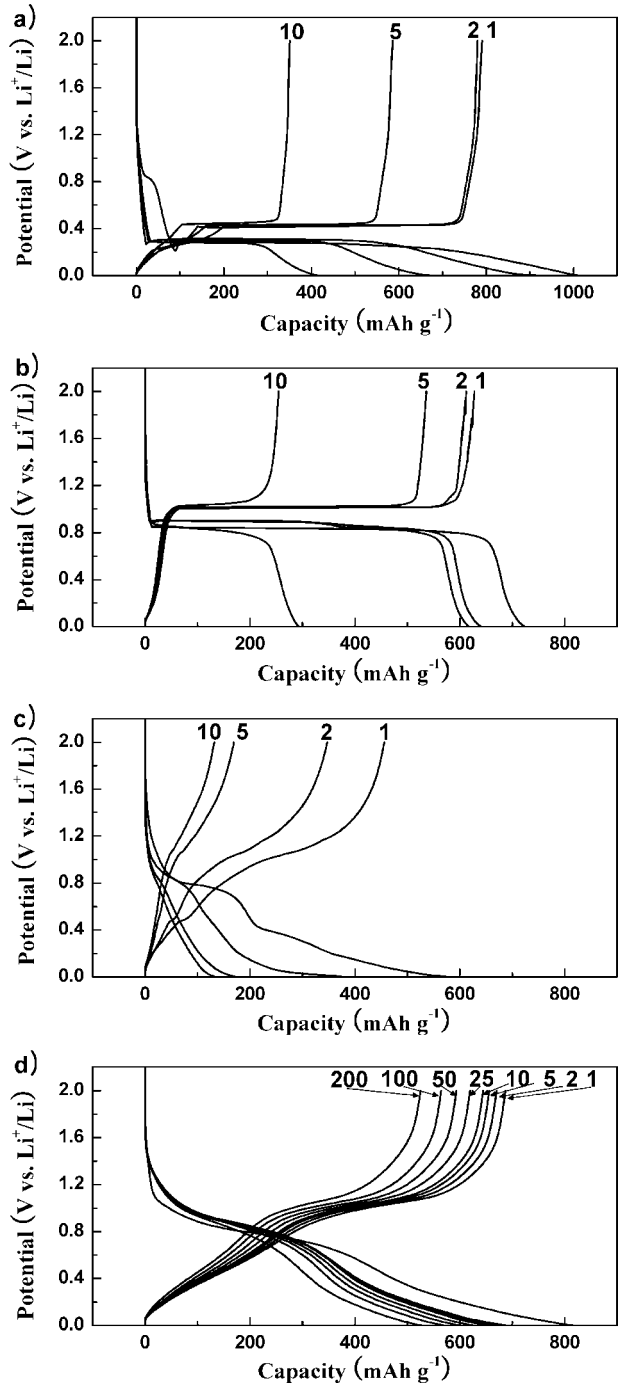

Figure 4. Electrochemical behavior of the four electrodes cycled between 0.0 and ~2.0 V vs Li$^+$/Li at a cycling rate of 100 mA g^{-1}: (a) aluminum, (b) antimony, (c) AlSb, and (d) Sb/Al$_4$C$_3$/C nanocomposite.

TEM bright-field and HRTEM images combined with selected-area diffraction (SAD) revealed the crystalline nanostructure of the AlSb particles formed by eq 1 (Figure 3a). Figure 3b shows TEM bright-field and HRTEM images combined with SAD patterns of the Sb/Al$_4$C$_3$/carbon nanocomposite formed by eq 2. The HRTEM image shows the uniform dispersion of the approximately 5 nm-sized Sb particles and amorphous Al$_4$C$_3$ in the amorphous carbon matrix. In Figure 3c, Sb, Al$_4$C$_3$, and carbon are well-dispersed within the composite, as shown by the EDS mapping image. It can be concluded that 100 to ~300 nm Sb/Al$_4$C$_3$/carbon

Table 1. Charge Capacity, Discharge Capacity, Coulombic Efficiency of First Cycle, and Cycle Retention for Al, Sb, AlSb, and Sb/Al_4C_3/C Nanocomposite Electrodes

electrode	first charge capacity (mAh g^{-1})	first discharge capacity (mAh g^{-1})	Coulombic efficiency (%)	cycle retention of discharge capacity (%)
Al	1010	791	78	44 (after 10 cycles)
Sb	723	628	87	41 (after 10 cycles)
AlSb	580	456	79	29 (after 10 cycles)
Sb/Al_4C_3/C	813	687	85	77 (after 200 cycles)

nanocomposite particles were composed of nanosized (about 5 nm) Sb, amorphous Al_4C_3, and amorphous carbon, as illustrated in Figure 3d.

The voltage profiles of the Al, Sb, AlSb, and Sb/Al_4C_3/carbon nanocomposite are shown in Figure 4a−d, respectively. The first charge and discharge capacities with a Coulombic efficiency for the first cycle of Al, Sb, AlSb, and the Sb/Al_4C_3/C nanocomposite electrode are presented, respectively, in Table 1. Pure Al, Sb, and AlSb electrodes demonstrated very poor cyclability. The drastic capacity decrease of the Al, Sb, and AlSb electrodes was caused mainly due to the large volume change associated with the pulverization of the active material and its electrical isolation from the current collector. The Coulombic efficiency of the Sb/Al_4C_3/carbon nanocomposite electrode for the first cycle was ~85%, confirming its very good electrochemical reversibility. Considering that the irreversible capacity of the milled carbon in the Sb/Al_4C_3/carbon nanocomposite was ~130 mAh g^{-1}, the enhanced cyclability and very good reversibility were attributed the well-distributed, nanosized Sb and amorphous Al_4C_3 in the amorphous carbon matrix.

The differential capacity plot (DCP, Figure 5a) of the first cycle of the Sb/Al_4C_3/carbon nanocomposite electrode shows two broad peaks during charging, along with two broad peaks during discharging. These peaks indicated that the Sb/Al_4C_3/carbon nanocomposite electrode has two electrochemical reactions corresponding to nanocrystalline Sb (corresponding to the broad peak near 0.8 V) and amorphous Al_4C_3 (corresponding to the broad peak around 0.2 V) with Li. Figure 5b,c shows electrochemical behavior of the Sb/C[15] and Al_4C_3/C composites with Li, respectively, for comparison. In the case of the Sb/C composite, the voltage for the reaction with Li matched that of the Sb/Al_4C_3/carbon nanocomposite electrode (dotted circles in Figure 5a,b). Although Wu reported the fabrication of amorphous Al_4C_3 by a simple mechanical milling technique,[25] we could not reproduce amorphous Al_4C_3 by the mechanical milling method. Alternatively, the reduced crystalline Al_4C_3/C composite was prepared by HEMM for 50 h, and the electrochemical behavior was compared to that of the Sb/Al_4C_3/carbon nanocomposite. Although most metal carbides do not react with Li,[11,26] the charge and discharge capacities of the Al_4C_3/C composite were 450 and 300 mAh g^{-1}, respectively, and good cyclability was demonstrated as shown in the inset graph of Figure 5c. The first irreversible capacity was mainly from the carbon in the Al_4C_3/C composite and solid electrolyte interface formation near 0.7 V (small peak in DCP, Figure 5c). The DCP of the reduced crystalline Al_4C_3/C composite is shown in Figure 5c. As indicated by the dotted square, the broad peaks between 0.35 and 0.0 V during charging and between 0.1 and 0.7 V during discharging were very similar to those of the Sb/Al_4C_3/carbon nanocomposite electrode. The peak broadening near the reaction voltage confirmed the low crystallinity of Sb and amorphous Al_4C_3 in the Sb/Al_4C_3/carbon nanocomposite.

These data agree well with the reported reaction mechanism that Sb reacted with Li to form Li_2Sb at 0.82 V followed by Li_3Sb at 0.79 V during the first charge and that the Li_3Sb phase was transformed directly into the Sb phase at 1.02 V during the discharge.[15] The reactions with Li at the Al electrode involved the formation of LiAl at 0.28 V during the first charge cycle and the reverse reaction at 0.42 V during the discharge cycle.[10,11]

Cycle performances were compared for the AlSb (voltage range of 0.0−2.0 V), Sb/Al_4C_3/carbon nanocomposite (volt-

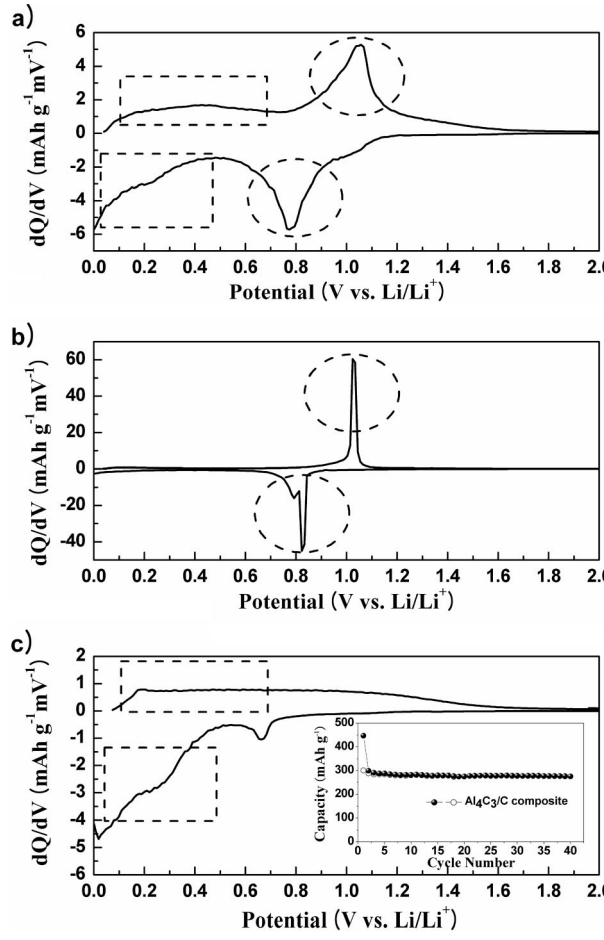

Figure 5. DCP of three electrodes: (a) Sb/Al_4C_3/C nanocomposite, (b) Sb/C composite, and (c) Al_4C_3/C composite (inset: cycling behavior of the Al_4C_3/C composite).

(25) Wu, N. Q. *J. Mater. Sci. Lett.* **1997**, *16*, 1810.
(26) Guo, Z. P.; Zhao, Z. W.; Liu, H. K.; Dou, S. X. *J. Power Sources* **2005**, *146*, 190.

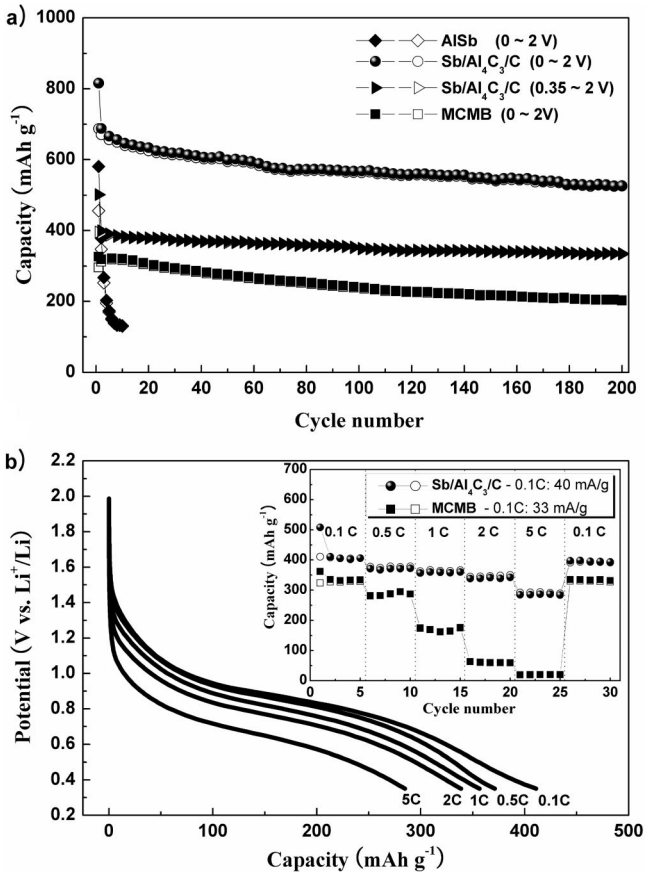

Figure 6. Cycling behaviors and C rate characteristics: (a) comparison of cycle performances for the Sb/Al$_4$C$_3$/C nanocomposite, AlSb, and MCMB at a cycling rate of 100 mA g^{-1}. (b) Voltage profiles at various C rates (inset: plot of charge capacity vs cycle number of the Sb/Al$_4$C$_3$/C nanocomposite and MCMB at various C rates).

age range of 0.0−2.0 and 0.35−2.0 V), and commercially available, mesocarbon microbead-graphite (MCMB, voltage range of 0.0−2.0 V) electrodes. As shown in Figure 6a, the cycle performance of the AlSb electrode was very poor. The capacity retention of the Sb/Al$_4$C$_3$/carbon nanocomposite showed a good electrochemical reversibility and good cyclability, as compared to that of the AlSb electrode, when it was cycled within the voltage range between 0.0 and 2.0 V. The Sb/Al$_4$C$_3$/carbon nanocomposite electrode showed a very stable capacity of approximately 520 mAh g^{-1} over 200 cycles, and the capacity retention of the discharge capacity of the first cycle was about 77%. When the electrode was cycled between 0.35 and 2.0 V (corresponding to the Li$_3$Sb and Sb phases, respectively), the test electrode showed a very good cycle performance with a capacity of more than 320 mAh g^{-1} over 200 cycles, and the capacity retention of the discharge capacity of the first cycle was about 85%. These good electrochemical characteristics were attributed to the uniform distribution of the nano Sb crystallite and amorphous Al$_4$C$_3$ phase and the buffering effect of the amorphous carbon matrix, as shown in Figure 3c.

The rate capability of the Sb/Al$_4$C$_3$/carbon nanocomposite electrode also was tested, and Figure 6b shows the cyclability of the Sb/Al$_4$C$_3$/carbon nanocomposite as a function of the C rate, with C being defined as the full use of the restricted charge capacity (400 mAh g^{-1}) in 1 h. The Sb/Al$_4$C$_3$/carbon nanocomposite electrode exhibited a high-rate capability. At rates of 2 and 5 C, the Sb/Al$_4$C$_3$/carbon nanocomposite electrode showed a very good charge capacity of 340 and 290 mAh g^{-1} with a stable cycling behavior, respectively. The rate capability of the Sb/Al$_4$C$_3$/carbon nanocomposite electrode was far better than that of the commercially used, MCMB-graphite, anode material, as shown in the inset of Figure 5b.

Conclusion

We developed a simple method for transforming micrometer-sized Al and Sb powders into a new nanocomposite modified with carbon by utilizing the alloying reaction of Al and Sb to form the AlSb phase and the dealloying reaction of the AlSb phase with carbon to synthesize the Sb/Al$_4$C$_3$/C nanocomposite using the HEMM technique without heat-treatment or chemical methods. When tested as an anode material for Li secondary batteries, this nanocomposite showed a highly reversible reaction with Li, a high discharge capacity of 687 mAh g^{-1} with a good Coulombic efficiency of 85% for the first cycle, and a high capacity above 520 mAh g^{-1} over 200 cycles. Additionally, by controlling the voltage window, an excellent cyclability with a high rate capability also was achieved. These excellent electrochemical properties demonstrated by the Sb/Al$_4$C$_3$/C nanocomposite electrode confirmed its potential as a new alternative anode material for Li-ion batteries. We anticipate that this simple transformation method for the conversion of micrometer-sized metal powders to their nanocomposites, utilizing alloying and dealloying reactions, will support their use in many other applications that require uniformly distributed, nanostructured, composite materials.

Acknowledgment. This work was supported by the Korea Science and Engineering Foundation (KOSEF) through the Research Center for Energy Conversion and Storage at Seoul National University (Grant R11-2002-102-02001-0).

CM800142N